Some Novel Binuclear Group 13 Metal Tin Hydrides Formed in Ar Matrices Following the Codeposition of the Metal Vapor with SnH_4

Benjamin Gaertner,[b] Hans-Jörg Himmel,*[b] Victoria A. Macrae,[a] Jennifer A. J. Pardoe,[a] Paul G. Randall,[a] and Anthony J. Downs*[a]

Abstract: IR measurements show that co-condensation of Al or Ga atoms (M) with SnH_4 in a solid Ar matrix at about 12 K results mainly in the spontaneous insertion of the metal into an Sn–H bond to form the M^{II} hydride $HMSnH_3$. Simultaneously the Ga_2 dimer also reacts with SnH_4, possibly to form a *nido*-type cluster $Ga_2(\mu\text{-}H)_4Sn$, with a metal-deficient cubane-like structure. All of these products are photolabile. Irradiation with visible light causes $HMSnH_3$ to tautomerize to the novel dihydrido-bridged species $H_2M(\mu\text{-}H)_2Sn$, which decomposes in turn under broad-band UV-visible light ($\lambda = 200$–800 nm); some $H_2Al(\mu\text{-}H)_2Sn$ is formed even on deposition. The data collected from experiments with SnH_4 and SnD_4 and different reagent concentrations, together with the results of quantum chemical calculations, are used to interpret the results and elucidate the structures and bonding of the new species.

Keywords: aluminum · gallium · hydrides · matrix isolation · stannanes · structure elucidation

Introduction

Activation of the E–H bond in hydride derivatives of a group 14 element E remains a primary issue, particularly for E = C or Si, attracting a huge investment of research effort.[1] To bring about such activation by insertion of a metal atom M into the E–H bond, it is necessary to design a compound of M that is able to bind more or less specifically to the formally saturated EH_n fragment of the hydride. There is, therefore, particular interest in the isolation of complexes in which an alkane or silane molecule is coordinated to a metal center, for example, $[Pt(CH_4)(Me)(H)_2(Tp)]$ (Tp = hydridotris(pyrazolyl)borate)[2] and $[(R_3P)_2(H)_2Ru(SiH_4)Ru(H)_2(PR_3)_2]$ (R = Cy or *i*Pr).[3] Of the well-characterized Group 14 hydrides, stannanes are the most polarizable and contain the most nucleophilic hydrogen atoms. In keeping with the expectation that they are therefore the most susceptible to complexation, several transition-metal complexes have indeed been characterized, not with stannane itself but with derivatives such as Ph_3SnH. The crystal structures of representative examples, namely $[Mn(\eta^5\text{-}MeC_5H_4)(CO)_2(HSnPh_3)]$[4] and $[Cr(\eta^6\text{-}$mesitylene$)(CO)_2(HSnPh_3)]$,[5] reveal η^2-coordination of the stannane through its Sn–H bond.

Relatively well established though transition-metal complexes are, interaction of a Group 14 hydride with an s- or p-block center is expected to be much weaker, and experimental evidence of complexation is sparse. In such circumstances matrix-isolation experiments[6,7] are often instructive, and indeed weak complexes of SiH_4 with both base (NH_3)[8] and acid (HF[9] and HONO[10]) partners have been successfully characterized in this way. Contact pairs $M\cdots SiH_4$ are undoubtedly formed when metal atoms M are co-condensed with an excess of SiH_4-doped Ar. When M is a Group 12 metal atom (Zn, Cd or Hg) in its ^1S ground electronic state, interaction with the SiH_4 is too weak to produce any detectable spectroscopic sign of complexation.[11] On the evidence of the IR, EPR, and UV-visible spectra, however, the Group 13 metal atoms Al and Ga form weakly bound, but spectroscopically distinct, 1:1 complexes in which the metal atom is η^2-coordinated by the SiH_4.[12–14] $^2S \leftarrow {}^2P$ or $^2D \leftarrow {}^2P$ excitation then results in insertion of the metal atom into an Si–H bond to form the M^{II} derivative $HMSiH_3$, a process which can be reversed by exchanging UV for visible photolyzing radiation ($\lambda \approx 580$ nm). By contrast with Ga atoms, though, the Ga_2 dimer in its ground electronic state ($^3\Pi_u$) inserts *spontaneously* into an Si–H bond of SiH_4, probably giving the SiH_3-bridged product $HGa(\mu\text{-}SiH_3)Ga$.[14]

[a] Dr. V. A. Macrae, Dr. J. A. J. Pardoe, P. G. Randall, Prof. A. J. Downs
Inorganic Chemistry Laboratory, University of Oxford
South Parks Road, Oxford OX1 3QR (UK)
Fax: (+44) 1865-272690
E-mail: tony.downs@chem.ox.ac.uk

[b] B. Gaertner, Priv.-Doz. Dr. H.-J. Himmel
Institut für Anorganische Chemie der Universität Karlsruhe
Engesserstrasse, Geb. 30.45, 76128 Karlsruhe (Germany)
Fax: (+49) 721-608-4854
E-mail: himmel@chemie.uni-karlsruhe.de

Supporting information for this article is available on the WWW under http://www.chemeurj.org/ or from the author.

  DOI: 10.1002/chem.200400564

The more polarizable SnH_4 molecule affords the prospect of a more complete spectroscopic characterization of an adduct with a Group 13 metal atom, with a correspondingly greater degree of pre-activation of one or more Sn–H bonds. The IR evidence we present here testifies, however, that co-deposition of Al or Ga (M) vapor with SnH_4 in an Ar matrix at approximately 12 K results in seemingly spontaneous insertion of the metal atom into an Sn–H bond to form the M^{II} hydride $HMSnH_3$ (**V**). At the same time, Sn–H bond activation is also effected by Ga_2 dimers, possibly with the formation of a hydrogen-bridged cluster $Ga_2(\mu\text{-}H)_4Sn$ (**VIII**). Irradiation with visible light causes tautomerization of **V** to a novel dihydrido-bridged species $H_2M(\mu\text{-}H)_2Sn$ (**VI**), which decomposes under broad-band UV-visible light ($\lambda = 200$–800 nm). The conclusions have been endorsed by the results of detailed density functional theory (DFT) calculations.

Experimental Section

Aluminum (Merck, purity 99.99%) was evaporated from a boron nitride cell heated resistively to about 1100°C, gallium (Aldrich, purity 99.9999%) from a tantalum cell similarly heated to about 900°C. The metal vapor was co-deposited with SnH_4 or SnD_4 and an excess of argon (used as supplied by Messer, purity 99.998%, or BOC, Research grade) on an appropriate support cooled to about 12 K by means of a closed cycle refrigerator (Leybold LB 510 or Air Products CS 202). For experiments with aluminum, carried out in Karlsruhe, the support was a highly polished copper block and IR spectra of the matrices were recorded in reflection;[15] for experiments with gallium, carried out in Oxford, the support was a CsI window and IR spectra were recorded in transmission.[16] The proportions SnH_4 (SnD_4)/Ar were typically between 0.1:100 and 1:100, while the deposition rate was approximately 1.0–1.5 mmol of matrix gas per hour, continued over a period of 0.5–1.5 h. The amount of deposited Al metal was measured with a quartz microbalance; rates of 5 $\mu g\,h^{-1}$ were chosen.

SnH_4 (SnD_4) was prepared by the reaction of $LiAlH_4$ ($LiAlD_4$) with $SnCl_4$ in diethyl ether and purified by repeated fractional condensation in vacuo;[17] the purity was checked by reference to the IR spectrum of the vapor.[18] Gas mixtures of Ar with SnH_4 or SnD_4 were prepared by standard manometric methods.

Photolysis was carried out with a medium-pressure Hg lamp (Philips LP 125) operating at 70 W or a high-pressure Hg-Xe lamp (Spectral Energy) operating at 800 W, IR radiation being absorbed by a water filter so as to minimize any heating effects. Irradiation involved either broad-band UV-visible light ($\lambda = 200$–800 nm) or, more selectively, the light delivered through an appropriate interference filter: $\lambda = 254$ nm (fwhh 10 nm), $\lambda = 405$ nm (fwhh 10 nm), $\lambda = 436$ nm (fwhh 11 nm), $\lambda = 580$ nm (fwhh 9 nm), and $\lambda = 700$ nm (fwhh 5 nm).

IR spectra recorded at Karlsruhe were measured in the range 4000–200 cm^{-1} with a Bruker 113v spectrometer operating with either a liquid N_2-cooled MCTB or a DTGS detector. Similar measurements at Oxford were made with a Nicolet Magna-IR 560 instrument. UV-visible spectra were recorded 1) with an Xe arc lamp (Oriel), an Oriel Multispec spectrograph and a photodiode-array detector for the Al experiments, or 2) with a Perkin–Elmer–Hitachi Model 330 spectrophotometer for the Ga experiments.

DFT calculations (using the BP86 functional in combination with a TZVPP basis set for Al, Ga, H and an ecp-TZVPP for Sn) were performed using the TURBOMOLE program suite.[19] Trial calculations showed that this methodology reproduces satisfactorily the observed geometry, dimensions, and IR spectrum of SnH_4.

Results

Progress of the thermally and photolytically initiated reactions of the metal vapor species with stannane was tracked and products were characterized principally with reference to the IR spectra of the Ar matrices supporting the reagents. The IR absorptions have been assigned and analyzed on the basis of the following criteria: 1) their growth or decay characteristics under different conditions, 2) comparisons with the spectra registered in control experiments and with the spectra of related species, and 3) the observed effects of exchanging SnH_4 for SnD_4 and of the different naturally occurring isotopes of Ga (^{69}Ga and ^{71}Ga).

Aluminum

IR spectra: Table 1 gives relevant details of the wavenumbers and growth/decay behavior of the IR spectra recorded in an experiment in which Al vapor was co-deposited with an excess of Ar doped with SnH_4 in the proportions 100:0.5. In addition to the absorptions characteristic of free SnH_4[18,20] and of trace impurities such as H_2O,[21] CO,[22] and CO_2,[23] the IR spectrum recorded immediately after deposition contained numerous absorptions associated with the product or products of spontaneous reactions involving Al atoms in their ground electronic state. Certain weak features could be identified with known products, for example, AlCO[24] and Al_2O,[25] formed from the metal atoms and impurities. The major features, falling in the regions 1730–1850, 1380–1430, 1100–1300, 700–750, 600–620, and 520–550 cm^{-1}, were attributable, however, to the outcome of reactions between Al atoms and SnH_4. Their profusion, while reflecting in part the occupancy by the guest species of different matrix sites, became accountable when the matrix was subsequently irradiated with light of selected wavelengths. In a typical sequence, photolysis was carried out first at $\lambda \approx 700$ nm, then successively at $\lambda \approx 580$ and 410 nm, and finally with broad-band UV-visible light ($\lambda = 200$–800 nm). The response of the IR spectrum to the different conditions revealed the formation of two major products, **1a** and **2a**, as well as at least one other species, believed to be a matrix-separated adduct Al···SnH_4, **3a**.

Photolysis with red light at $\lambda \approx 700$ nm brought about the rapid decay of a family of bands with the following wavenumbers: 1839.3, 1830.6, 1821.7, 1774.8, 728.1, 720.3, and 657.8 cm^{-1} (see Figure 1). These we associate with the primary product (**1a**) of a spontaneous reaction between Al atoms and SnH_4. The bands occurring in the range 1730–1850 cm^{-1}, on the low-wavenumber flank of the antisymmetric ν(Sn–H) fundamental of SnH_4, ν_3 (t_2), are likely to arise from the stretching vibrations of terminal Sn–H[18,20,26] or Al–H[26,27] bonds. The others, near 720 cm^{-1}, come close to the scissoring, ν_2 (e), and antisymmetric bending, ν_4 (t_2), fundamentals of SnH_4.[18]

The decay of the IR signals due to **1a** was accompanied by the growth of a second family of bands already evident in the spectrum of the matrix prior to photolysis. Characterized by multiplet patterns in several cases and centered near 1880, 1400, 1260, 1220, 1130, 733, 612, and 535 cm^{-1}, these

Table 1. IR absorption wavenumbers [cm^{-1}] observed for an Ar matrix containing Al/SnH_4 or Al/SnD_4 mixtures at 12 K.

SnH_4	SnD_4	H/D ratio	Dep[a]	700[a]	410[a]	Bb[a]	Species
1878.1	1390.1	1.3510	↑	↑	↑	↓	**2a**
1854.7/1853.1			↑	–	↓	–	**3a**
1845.0			↑	–	↓	–	**3a**
1839.3	1321.6	1.3951	↑	↓	–	–	**1a**
1835.3/1833.9			↑	–	↓	–	**3a**
1830.6	1316.2	1.3704	↑	↓	–	–	**1a**
1821.7	1307.9	1.3605	↑	↓	–	–	**1a**
1812.6			–	–	–	↑	[b]
1774.8	1292.6	1.3513	↑	↓	–	–	**1a**
1633.7			↑	–	–	↓	[b]
1630.2			↑	–	–	↓	[b]
1612.0			↑	–	–	↓	[b]
1424.9			↑	–	–	↓	[b]
1414.5/1400.1	1010.3	1.3858	↑	↑	↑	↓	**2a**
1408.8			↑	–	–	↓	[b]
1277.4/1271.4/1246.8	922.7	1.3730	↑	↑	↑	↓	**2a**
1238.2/1209.6	889.1	1.3928	↑	↑	↑	↓	**2a**
1234.4			↑	–	–	↓	[b]
1129.1			↑	↑	↑	↓	**2a**
1121.2			↑	–	–	↓	[b]
1113.8			↑	–	–	↓	[b]
755.9			↑	–	↓	–	**3a**
732.9	534.8	1.3908	↑	↑	↑	↓	**2a**
728.1			↑	↓	–	–	**1a**
720.3			↑	↓	–	–	**1a**
705.1			–	↑	–	↓	[b]
657.8	471.5	1.3917	↑	↓	–	–	**1a**
611.5			↑	↑	↑	↓	**2a**
541.2/528.6			↑	↑	↑	↓	**2a**

[a] Dep = on deposition; 700 = 700 nm photolysis; 410 = 410 nm photolysis; Bb = broad-band UV-visible photolysis. [b] unknown product.

modest activation barrier. At the lowest SnH_4 concentration (Ar/SnH_4 = 100:0.02) it was possible to descry very close to the ν_3 absorption of free SnH_4 an additional feature at 1878.0 cm^{-1} also belonging to **2a** (see Figure 2). Most distinctive of the IR absorptions due to **2a** are those appearing in the range 1100–1430 cm^{-1}, suggesting by their wavenumbers the stretching vibrations of one or more M-H-M′ bridges, where M and M′ may be the same or different metal atoms (cf. $H_2Al(\mu\text{-}H)_2AlH_2$ 1408/1268[28] and $Me_2Al(\mu\text{-}H)_2AlMe_2$ 1353/1215 cm^{-1}[29]).

While irradiation at wavelengths near 700 nm brought about the decay of the bands due to **1a**, it had no effect on a third family of significantly weaker bands that was present at the outset. With wavenumbers of 1854.7/1853.1, 1845.0, 1835.3/1833.9 and 755.9 cm^{-1} (see Figure 1), these are associated with a species **3a** showing the spectroscopic characteristics to be expected of a perturbed SnH_4 molecule. Yet a fourth family of weak bands at 1633.7, 1630.2, 1612.0, 1424.9, 1408.8, 1234.4, 1121.2, and 1113.8 cm^{-1}, also present

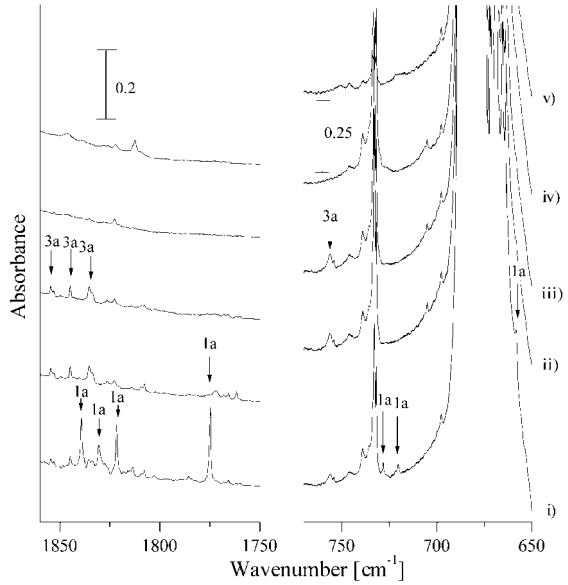

Figure 1. IR spectra showing the reactions of Al atoms in an Ar matrix containing 0.5% SnH_4: i) following deposition, ii) following photolysis at $\lambda \approx 700$ nm, iii) following photolysis at $\lambda \approx 580$ nm, iv) following photolysis at $\lambda \approx 410$ nm, and v) following broad-band photolysis at $\lambda = 200$–800 nm. Regions relevant to products **1a** and **3a**.

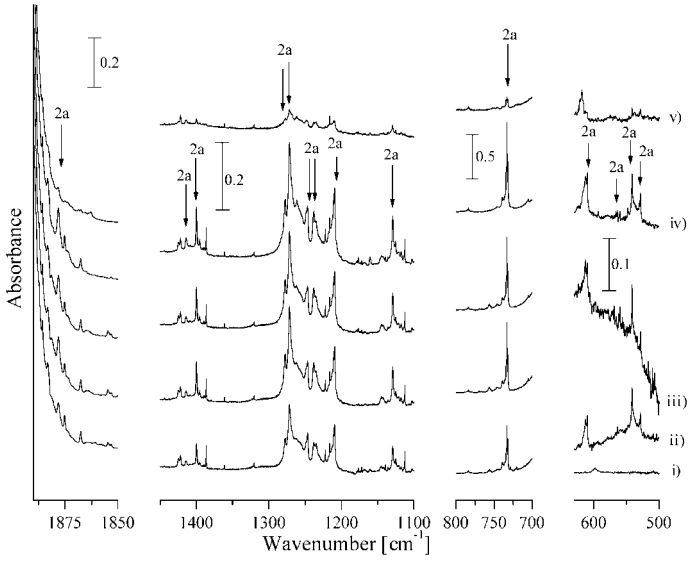

Figure 2. IR spectra showing the reactions of Al atoms in an Ar matrix containing 0.5% SnH_4: i) following deposition, ii) following photolysis at $\lambda \approx 700$ nm, iii) following photolysis at $\lambda \approx 580$ nm, iv) following photolysis at $\lambda \approx 410$ nm, and v) following broad-band photolysis at $\lambda = 200$–800 nm. Regions relevant to product **2a**.

denote a second major product (**2a**) of the reaction between Al atoms and SnH_4 formed either thermally or, more probably, photolytically with the surmounting of a comparatively

at the outset, were likewise unaffected by 700 nm radiation. The carrier of this family we have been unable to identify positively, although the wavenumbers and photochemical response of the bands suggest an adduct of **2a** and H_2O impurity.

Subsequent photolysis with light of $\lambda \approx 580$ nm gave rise to minimal changes in the IR spectrum of the matrix. On the other hand, switching the wavelength of the photolyzing radiation to $\lambda \approx 410$ nm caused the absorptions identified with **3a** to decay, while those due to **2a** gained somewhat in intensity. It was noted, too, that irradiation at $\lambda \approx 580$ and 410 nm induced some minor changes in the relative intensities of the components of the complex multiplets near 1880, 1400, 1200, and 1100 cm^{-1} associated with **2a**. Completion of the period of photolysis at $\lambda \approx 410$ nm left **2a** and the unidentified product as the sole surviving matrix guests. That these, too, are photolabile was then demonstrated by a final stage in which the matrix was exposed to broad-band UV-visible radiation ($\lambda = 200$–800 nm) and resulting in the near-extinction of the IR signatures of both products. Photodecomposition was accompanied, however, neither by the appearance of any new IR bands of significant intensity nor by the reappearance of the bands associated with **1a** or **3a**. Of the known binary hydrides AlH_n[27] and SnH_n[20] there was also no sign for $n = 1$–3.

Raising the SnH_4 concentration added to the complexity of the spectra by introducing additional satellites to some of the absorptions identified with the products **1a**–**3a** that are attributable presumably to matrix site effects. Nevertheless, there was a more or less proportionate increase in the intensities of the initial product bands, implying that a single SnH_4 molecule enters into the reactions affording **1a**, **2a**, and **3a**. Increasing the metal concentration by raising the furnace temperature led to a similar increase in intensity of all the relevant absorptions, causing us to infer that the products **1a**–**3a** all derive from interaction of Al atoms with SnH_4 in the proportions 1:1.

As illustrated in Figure 2, many of the IR bands characterizing **2a** appeared as multiplets reflecting most probably the influence of different trapping sites on a highly deformable and/or reactive molecule, compare with $Ga(\mu\text{-}H)_2Ga$ in similar circumstances.[30] Systematic studies located the multiplet component corresponding in most cases to the *main* trapping site, and for the sake of simplicity, the rest of the discussion will refer only to these wavenumbers (as in Table 6, see later). Experiments in Kr matrices gave no advantage, resulting only in broad product absorptions.

Analogous experiments were carried out with SnD_4 in place of SnH_4, with the results included in Table 1; representative IR spectra are shown in Figures 3 and 4. Again, product absorptions were observed in the spectrum recorded immediately after deposition of the matrix, and these could be attributed satisfactorily to perdeuterated versions of the products **1a**, **2a**, and **3a** on the basis of their response to different conditions of photolysis. All the features were strongly red-shifted with respect to their identifiable counterparts

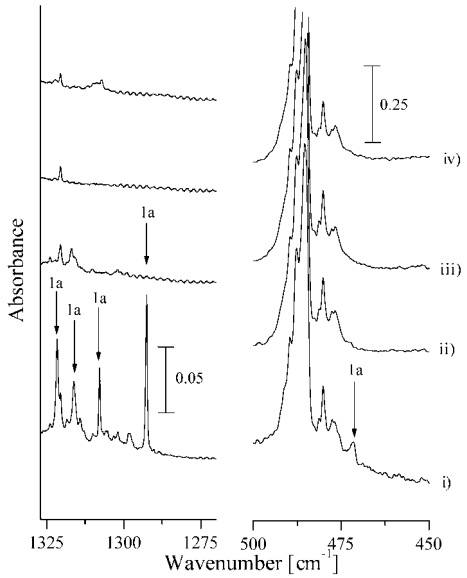

Figure 3. IR spectra showing the reactions of Al atoms in an Ar matrix containing 0.5% SnD_4: i) following deposition, ii) following photolysis at $\lambda \approx 700$ nm, iii) following photolysis at $\lambda \approx 410$ nm, and iv) following broad-band photolysis at $\lambda = 200$–800 nm. Regions relevant to product **1a**.

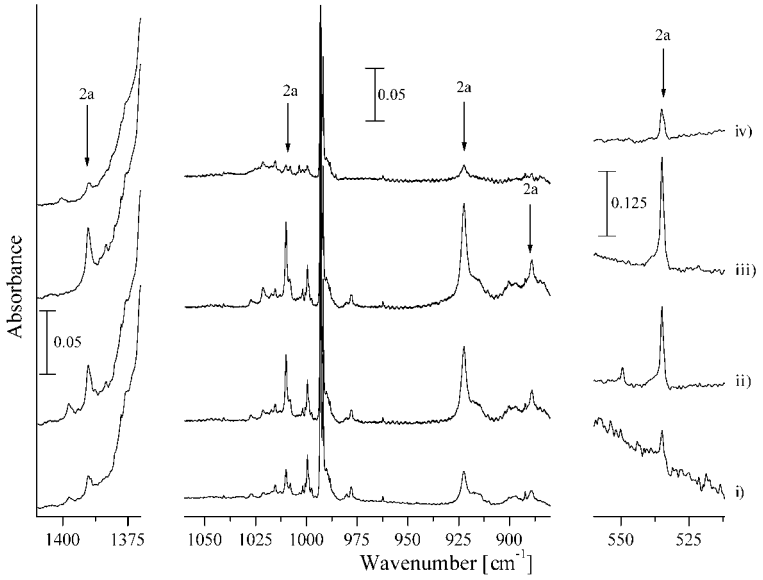

Figure 4. IR spectra showing the reactions of Al atoms in an Ar matrix containing 0.5% SnD_4: i) following deposition, ii) following photolysis at $\lambda \approx 700$ nm, iii) following photolysis at $\lambda \approx 410$ nm, and iv) following broad-band photolysis at $\lambda = 200$–800 nm. Regions relevant to product **2a**.

for the isotopically natural forms of the molecules. The bands due to **1a** at 1730–1850 cm^{-1} moved on deuteration to 1280–1330 cm^{-1}, giving H/D ratios near 1.392:1 for each of the three main features at higher wavenumber, but 1.3730:1 for the most prominent feature at 1774.8/1292.6 cm^{-1}. The reduced H/D ratio, combined with the wavenumbers themselves, lends some weight to the assignment of this last transition not to a ν(Sn–H) but to the ν(Al–H) fundamental of an Al^{II} hydride (cf. HAlH 1806.3/1769.5,[27] $HAlCH_3$ 1764/1746,[31] $HAlSiH_3$ 1780.9,[13,14] $HAlNH_2$ 1761.1,[32] and $HAlPH_2$ 1768.2 cm^{-1}[33]). The band of isotopically natural **1a** at 657.8 cm^{-1} shifted on deuteration to 471.5 cm^{-1} (H/D = 1.3951:1). Similar shifts were noted for **2a**. Thus, the transitions near 1880, 1400, 1210, 1130, and 733 cm^{-1} moved to 1390, 1010, 923, 889, and 535 cm^{-1}, respectively, giving H/D ratios ranging from 1.386:1 to 1.270:1. The measured IR properties of the deutero version of **3a** were consistent with the behavior expected of vibrations localized within an SnH_4 (SnD_4) fragment.

UV-visible spectra: UV-visible spectra of Ar matrices doped with Al vapor and SnH_4 showed no bands belonging to any species other than Al atoms[34,35] or Al_2 dimers.[36] Recording IR and UV-visible spectra of the same matrix for different Al concentrations served to validate the assumption that products **1a** to **3a** each contain only one Al atom.

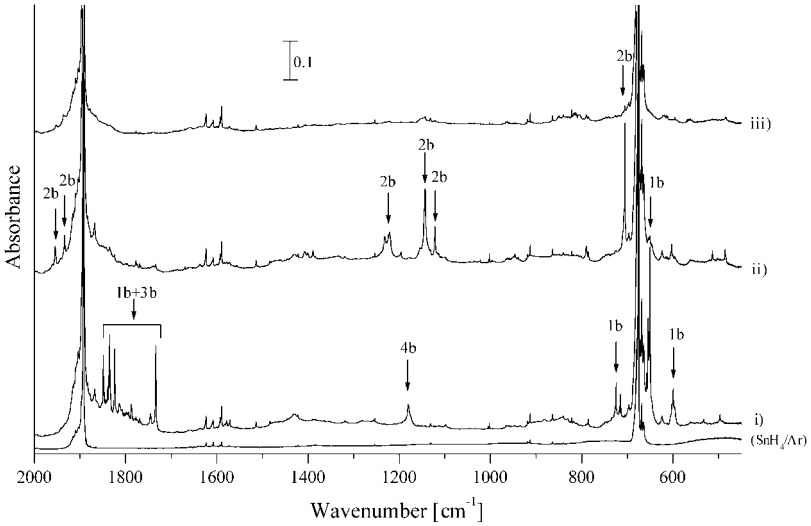

Figure 5. IR spectra showing the reactions of Ga vapor species in an Ar matrix containing 0.15 % SnH_4: i) following deposition, ii) following photolysis at $\lambda \approx 405$ nm, and iii) following broad-band photolysis at $\lambda = 200$–800 nm.

Table 2. IR absorption wavenumbers [cm^{-1}] observed for an Ar matrix containing Ga/SnH_4 or Ga/SnD_4 mixtures at 12 K.

SnH_4	SnD_4	H/D ratio	Dep[a]	577[a]	405[a]	Bb[a]	Species
1961.2/1954.8	1390.9/1389.1	1.4086		↑	↑	↓	**2b**
1934.3	1375.7	1.4060		↑	↑	↓	**2b**
1849.3	1328.5/1324.5/1322.8/1320.4	1.3967	↑	↓	↓	↓	**1b**
1839.4	1305.5	1.4090	↑	[b]	↓	↓	**3b**
1835.3	1309.3/1301.0	1.4062	↑	↓	↓	↓	**1b**
1824.7	1288.4	1.4163	↑	↓	↓	↓	**1b**
1813.5			↑	↓	↓	↓	**1b**
1787.8	1281.4/1278.4	1.3968	↑	[b]	↓	↓	**3b**
1746.4	1269.8	1.3753	↑	[c]	↓	↓	[d]
1734.4	1253.3	1.3839	↑	↓	↓	↓	**1b**
1669.9	1215.2	1.3742			↑	↓	HGaOH[e]
1407.7/1401.2/1389.6	1008.6/998.7	1.3957		↑	↑	↓	**2b**
1232.5/1221.2/1196.5	888.2/882.7/867.8/864.3	1.3835		↑	↑	↓	**2b**
1180.3	857.3	1.3768	↑	[b]	↓	↓	**4b**
1144.1	830.9/829.2	1.3769		↑	↑	↓	**2b**
1122.0	811.1/808.2	1.3833		↑	↑	↓	**2b**
1002.2			↑	↓	↓	↓	Ga_2H_2[f]
724.8	516.1	1.4044	↑	↓	↓	↓	**1b**
714.8	511.0/509.1	1.4014	↑	↓	↓	↓	**1b**
704.8	505.6	1.3940		↑	↑	↓	**2b**
654.4/650.4	469.2/466.2	1.3949	↑	↓	↓	↓	**1b**
615.7	438.2/436.9	1.4072		↑	↑	↓	**2b**
602.4/599.4	430.5	1.3958	↑	[c]	↓	↓	[d]
514.0				↑	↑	↓	**2b**
496.8			↑	↓	↓	↓	**1b**
485.8				↑	↑	↓	[d]

[a] Dep = on deposition; 577 = 577 nm photolysis; 405 = 405 nm photolysis; Bb = broad-band UV-visible photolysis. [b] Decreases but little. [c] Decreases rapidly. [d] Unknown product. [e] See reference [43]. [f] See reference [30].

Gallium

IR spectra: Figure 5 depicts the IR spectra recorded in an experiment in which Ga vapor was co-deposited with an excess of Ar doped with 0.15 % SnH_4; relevant details of wavenumbers and growth/decay characteristics are itemized in Table 2. On deposition, the matrix exhibited in addition to the absorptions associated with SnH_4[18,20] and the usual trace impurities[21–23] numerous new features attributable to the product or products of spontaneous reactions between SnH_4 and either Ga atoms or Ga_n clusters in their ground electronic states. Several occurred in the range 1720–1860 cm^{-1}, thereby suggesting their origin in the stretching vibrations of terminal Sn–H[18,20,26] or Ga–H[26,27] bonds. Others, near 720 and 660 cm^{-1}, came close to the scissoring, ν_2 (e), and antisymmetric bending, ν_4 (t_2), fundamentals of

SnH_4.[18] The spectrum was significantly simpler, however, than that observed in similar circumstances in experiments with Al vapor. It included, for example, only one absorption in the range 800–1700 cm^{-1}, this occurring at 1180.3 cm^{-1}.

Subsequent photolysis treatments brought to light further differences between the behaviors of Al and Ga toward SnH_4. Thus, irradiation with light at $\lambda \approx 700$ nm had no detectable effect on the products formed on co-condensation of Ga and SnH_4. Moving the wavelength of the photolyzing radiation to $\lambda \approx 580$ nm (see Figure 6) did, however, result in

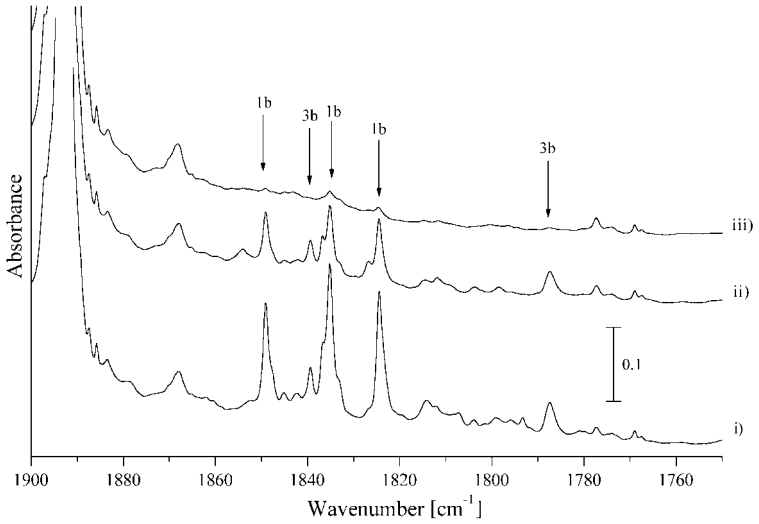

Figure 6. IR spectra showing the reactions of Ga vapor species in an Ar matrix containing 0.15% SnH_4: i) following deposition, i) following photolysis at $\lambda \approx 577$ nm, and iii) following photolysis at $\lambda \approx 405$ nm.

the decay of most of the new bands, some more quickly than others. On the basis of numerous experiments and careful scrutiny of the growth and decay patterns, it was possible to identify absorptions with the following wavenumbers with the main product formed on co-deposition of the metal vapor with SnH_4: 1849.3, 1835.3, 1824.7, 1813.5, 1734.4, 724.8, 714.8, 654.4/650.4, and 496.8 cm^{-1}. The most intense feature was that near 650 cm^{-1}. Despite the higher energy threshold to photodecomposition, the conditions of formation and spectroscopic properties gave every reason to label the associated product **1b**, that is, the Ga analogue of **1a**. Weak signals at 1746.4 and 602.4/599.4 cm^{-1} decayed much more quickly than did the bands already identified with **1b**, whereas others, located at 1839.4, 1787.8, and 1180.3 cm^{-1}, suffered little change of intensity. This behavior pointed to the presence of more than one product in the initial deposit, although the trapping of a molecule in different matrix sites can have a significant effect on its apparent photolability.[37] Such an effect may well be responsible, for example, for the behavior of the bands at 1746.4 and 602.4/599.4 cm^{-1}, which we tentatively ascribe to **1b** housed in a photoactivating matrix site. We believe, nevertheless, that at least two more products are present initially, namely **3b**, associated with the transitions at 1839.4 and 1787.8 cm^{-1}, and **4b** (lacking an Al counterpart), associated with the 1180.3 cm^{-1} transition. As in the experiments with Al, there was no sign of the photoreversible behavior displayed by the products $M\cdots SiH_4$ and $HMSiH_3$ (M = Al or Ga) formed by M atoms and SiH_4 under comparable conditions.[13,14]

Simultaneously with the progressive depletion of the matrix in **1b** new IR absorptions belonging to a common product were observed to develop. These were located at 1961.2/1954.8, 1934.3, 1407.7/1401.2/1389.6, 1232.5/1221.2/1196.5, 1144.1, 1122.0, 704.8, 615.7, and 514.0 cm^{-1}, with those at 1144.1 and 704.8 cm^{-1} being the most intense. The high wavenumber transitions at 1930–1965 cm^{-1} are noteworthy for appearing in a region typically associated with the ν(Ga–H) modes of Ga^{III} hydrides (cf. GaH_3 1923.2,[27] H_2GaNH_2 1970.8,[32] H_2GaCl 1978.1/1946.4,[38] and $H_2Ga(\mu\text{-}H)_2BH_2$ 2005/1982 cm^{-1}[39]). The strong absorptions appearing in the range 1120–1410 cm^{-1} find an evident parallel with the spectrum of **2a**, suggesting by their wavenumbers the stretching vibrations of bridging metal-hydrogen bonds (cf. $Ga(\mu\text{-}H)_2Ga$ 1002/906.5,[30] $H_2Ga(\mu\text{-}H)_2GaH_2$ 1273/1202,[40] and $Me_2Ga(\mu\text{-}H)_2GaMe_2$ 1290/1185 cm^{-1}[41]). The IR kinship to **2a** and the circumstances of formation (from **1b**) lead us to identify the new compound as **2b**, that is, the Ga analogue of **2a**. On the basis of its wavenumber, the only IR marker clearly attributable to product **4b** (at 1180.3 cm^{-1}) also implies the presence of one or more metal-hydrogen-metal bridges.

Exposing the matrix to light with $\lambda \approx 405$ or 436 rather than 580 nm, for example, for 30 min, led to much more rapid extinction of the bands due to **1b**, as well as the concomitant build-up of those due to **2b**. Such photolysis was also less selective in that it resulted in the decay of *all* the bands associated with the products formed on co-deposition of the Ga vapor with SnH_4, including **3b** and **4b**. However, these changes were not accompanied by the appearance of any new product signal. Subsequent irradiation with broadband UV-visible light (λ = 200–800 nm) had the effect of eliminating all traces of the products **1b**–**4b**, as well as the weaker features that have not been definitely assigned. No new IR absorptions of significant intensity were observed to grow in as a result. At neither this nor any earlier stage did the IR spectrum suggest the formation of a binary hydride of gallium, for example, GaH, GaH_2, GaH_3, or Ga_2H_6,[27,40] or subvalent tin, for example, SnH, SnH_2, or SnH_3,[20] previously characterized in varying degrees of detail. Annealing the matrix at temperatures up to about 30 K had little effect on its IR spectrum at either this or any earlier stage of its history.

Varying the metal and SnH_4 concentrations brought about such changes in intensity of the IR bands as to imply that **1b**, **2b** and **3b** each derive from a 1:1 stoichiometric reac-

tion of Ga atoms with SnH_4, but that **4b** is the product of a spontaneous reaction of Ga_2 with SnH_4. Such a conclusion is supported by the experience of other matrix studies in which the Ga_2 dimer has been implicated.[14,30]

Analogous experiments were carried out with SnD_4 in place of SnH_4, with the results included in Table 2 and illustrated in a typical experiment in Figure 7. Despite the com-

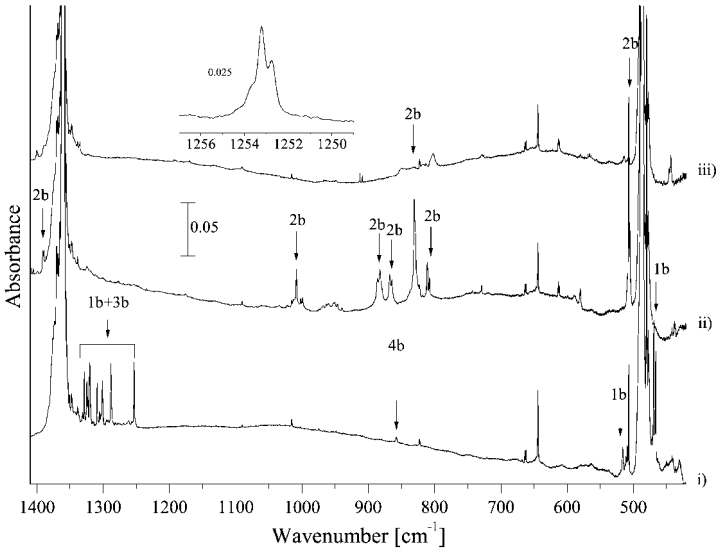

Figure 7. IR spectra showing the reactions of Ga vapor species in an Ar matrix containing 0.15% SnD_4: i) following deposition, ii) following photolysis at $\lambda \approx 405$ nm, and iii) following broad-band photolysis at $\lambda = 200$–800 nm. Inset: IR absorption at 1253.3 cm^{-1} as measured under a resolution of 0.125 cm^{-1}.

plications created in some cases by what appear to be matrix site effects (which are even more marked than in the experiments with SnH_4), the product absorptions observed on deposition could be attributed satisfactorily to perdeuterated versions of the products **1b**, **3b**, and **4b** on the basis of the effects of changing the metal concentration and conditions of photolysis. All the features were strongly red-shifted with respect to their counterparts for the isotopically natural forms of the molecules. Deutero analogues of all the main features associated with **2b** were likewise identified after photolysis with visible radiation, giving H/D ratios ranging from 1.3784:1 to 1.4101:1.

The bands due to **1b** at 1730–1850 cm^{-1} moved on deuteration to 1250–1330 cm^{-1}, giving H/D ratios of 1.3839–1.4163:1; those near 720 and 650 cm^{-1} were relocated to about 515 and 470 cm^{-1}, respectively, also corresponding to H/D ratios near 1.40:1. Similar shifts were noted for the features associated with **3b** and **4b**. Thus, for example, the single band at 1180.3 cm^{-1} marking **4b** moved to 857.3 cm^{-1} on deuteration, giving H/D = 1.3768:1, consistent with its attribution to the stretching vibration of an M-H-M′ bridge (M, M′ = Ga or Sn, being either the same or different atoms). The lower value of the H/D ratio (1.3839:1) shown by the intense absorption at 1734.4 cm^{-1} for the isotopically natural form of **1b** suggests that it may arise from a ν(Ga–H) rather than a ν(Sn–H) mode. Since there is more motion of the metal atom M in a ν(M–D) than in a ν(M–H) vibration, we have scrutinized the corresponding band at 1253.3 cm^{-1} in the spectrum of the perdeuterated version of **1b**. Under a resolution of 0.125 cm^{-1}, this could be seen, as illustrated in Figure 7, to be a doublet with components having relative intensities of roughly 3:2 and separated by 0.45 cm^{-1} (reflecting well the natural abundances of ^{69}Ga (60.1%) and ^{71}Ga (39.9%)[42] and the splitting of 0.5 cm^{-1} calculated for the stretching of a diatomic Ga–D unit).

UV-visible spectra: With low furnace temperatures (850 °C), the 300–900 nm range of the UV-visible spectrum of a matrix doped with the metal vapor and SnH_4 displayed, in addition to a sharp absorption at 342 nm corresponding to the $^2S \leftarrow {}^2P$ transition of atomic Ga,[7,16,34] a new absorption centered at 400 nm, the intensity of which showed a first-order dependence on the SnH_4 concentration. Photolysis of the matrix with radiation at $\lambda \approx 405$ nm caused this absorption to decay. Simultaneously a new absorption appeared to develop near 320 nm, accompanied by a weak, broader feature centered at 460 nm (see Figure S1, Supporting Information). IR spectra measured under the same conditions witnessed the initial formation of **1b** and **3b** with only low concentrations of **4b**, followed by the photochemical conversion of **1b** to **2b**. Raising the furnace temperature (to 900 °C) gave matrices whose UV-visible spectrum included initially not only the 342 and 400 nm bands, with proportionately enhanced intensities, but also a third band at 610 nm, weaker and broader than the other two, which has been identified previously[36] as arising from the Ga_2 dimer. The IR spectra measured under these conditions showed intensification of all the product signals, but of those due to **4b** conspicuously more than those due to **1b** and **2b**. Hence the measurements uphold the view that **1b**, **2b**, and **3b** are monogallium products, whereas **4b** is a digallium product. The new features at 400 and 320/460 nm are associated presumably with the principal products **1b** and **2b**, respectively. There is a superficial analogy between the first of these and the UV-visible transition characteristic of a weakly bound adduct involving a Ga atom, such as Ga···NH_3 (440 nm),[32] Ga···OH_2 (395 nm),[43] and Ga···SiH_4 (ca. 350 nm).[14]

Discussion

In the following account, we describe the results of detailed DFT calculations on model molecules. By considering the energies of plausible species, comparing the IR spectra simulated for these with the spectra observed for the various products, and taking into account all of the experimental circumstances, we are led to identify the main products as $HMSnH_3$ (**1a** or **1b**; **V**) and, surprisingly, its novel dihydrido-bridged tautomer, $H_2M(\mu\text{-}H)_2Sn$ (**2a** or **2b**; **VI**) for M = Al or Ga. We consider also the properties expected of the metal atom adduct M(^{2}P)···SnH_4 (**I**–**IV**) and suggest a matrix-frustrated version of this as probably accounting for the secondary product **3a** or **3b**, while the digallium product **4b** is most likely to be a hydrogen-bridged cluster $Ga_2(\mu$-

$H)_4Sn$ (**VIII**). The relevant reactions are then represented by Equations (1)–(4) in which M = Al or Ga.

$$M(^2P) + SnH_4 \rightarrow M(^2P)\cdots SnH_4 \quad (\mathbf{3a}, \mathbf{3b}) \qquad (1)$$

$$M(^2P) + SnH_4 \rightarrow HMSnH_3 \quad (\mathbf{1a}, \mathbf{1b}) \qquad (2)$$

$$HMSnH_3 \rightarrow H_2M(\mu\text{-}H)_2Sn \quad (\mathbf{2a}, \mathbf{2b}) \qquad (3)$$

$$Ga_2 + SnH_4 \rightarrow Ga_2(\mu\text{-}H)_4Sn \quad (\mathbf{4b}) \qquad (4)$$

M···SnH_4 (I–IV) and $HMSnH_3$ (V), (M = Al or Ga): The IR signatures of the products **1a** and **1b** and **3a** and **3b** show an evident kinship to that of their SnH_4 parent and all the features could reasonably be ascribed on the basis of their wavenumbers to either stretching or deformation of an SnH_n fragment, with the multiplicity of transitions suggesting the absence of anything higher than a twofold axis of symmetry. In line with expectations based on the results of similar matrix experiments with, for example, NH_3,[32] H_2O,[43] and SiH_4,[14] it might reasonably be assumed that the product **1** and/or **3** is a 1:1 adduct of the form $M(^2P)\cdots SnH_4$ (**I–IV**). Analogies with the behavior of SiH_4 have led to DFT calculations being carried out to establish minimum energy structures, in the first place for the possible isomers **I–III** illustrated in Figure 8. The geometries here differ according to whether the metal atom is located above the centroid of one of the faces (**I**), near a vertex (**II**), or above the midpoint of one of the edges (**III**) of the SnH_4 tetrahedron.

For both Al and Ga each in their ground electronic states [$M(^2P)$], DFT calculations find minima for models **I–III** with binding energies that follow the same order **I** < **II** < **III** as the analogous SiH_4 species.[14] However, when the models were allowed to assume unrestrained geometry, a more stable structure was found with the M atom placed above an Sn–H bond, which may thus be regarded as η^2-coordinated to M. In this structure, **IV**, the (η^2-HSn)M unit is coplanar with a second Sn–H bond to which M is proximal. The energy change for the reaction given in Equation (1), in which M···SnH_4 represents each of the isomers **I–IV**, is shown underneath the relevant geometries in Figure 8. Thus

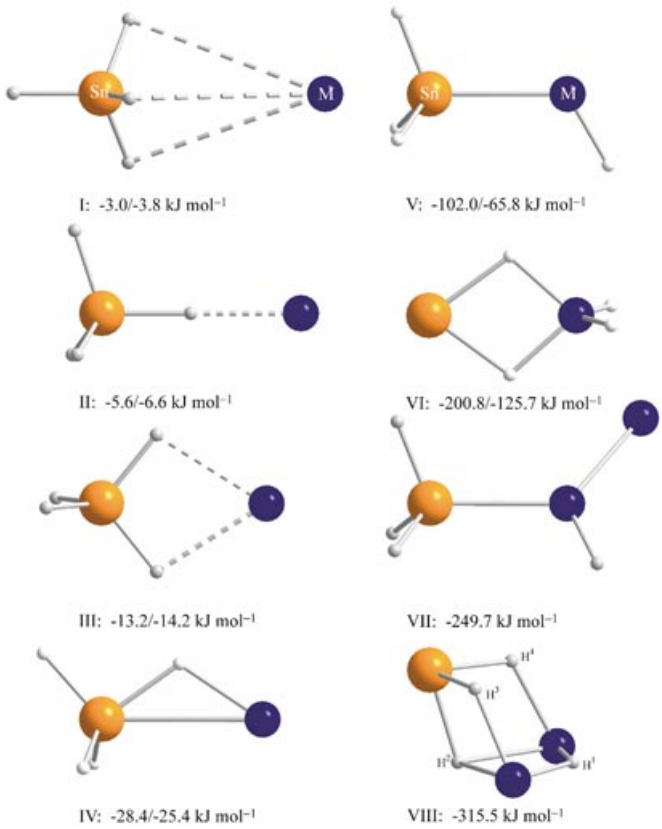

Figure 8. Geometries of possible isomers of the adduct M·SnH_4 (**I–IV**) and the molecules $HMSnH_3$ (**V**), $H_2M(\mu\text{-}H)_2Sn$ (**VI**), $GaGa(H)SnH_3$ (**VII**), and $Ga_2(\mu\text{-}H)_4Sn$ (**VIII**). Energies relate to ΔE for the change $M(^2P) + SnH_4 \rightarrow MSnH_4$ or $2M(^2P) + SnH_4 \rightarrow M_2SnH_4$.

IV is calculated to correspond to the global minimum with a binding energy of 28.4 kJ mol^{-1} for M = Al and 25.4 kJ mol^{-1} for M = Ga; it lies to low energy of **III** by 15.2 (Al) and 11.3 kJ mol^{-1} (Ga). The binding energy estimated at a similar level of theory for M···SiH_4 in its preferred form (analogous to **III**) is near 12 kJ mol^{-1}, irrespective of whether M = Al or Ga.[14]

Tables 3 and 4 list the wavenumbers and IR intensities predicted for the vibrational fundamentals, alongside details of the IR spectra observed for the products **1a**/**1b** and **3a**/

Table 3. Experimental IR wavenumbers [cm^{-1}] of **1a** and **3a** and calculated wavenumbers [cm^{-1}] and intensities [km mol^{-1}, given in parentheses] of the four isomers of Al·SnH_4, **I-IV**, and $HAlSnH_3$, **V**.

Observed		Al·SnH_4 (**I**)		Al·SnH_4 (**II**)		Al·SnH_4 (**III**)		Al·SnH_4 (**IV**)		$HAlSnH_3$ (**V**)	
1a	**3a**	Assign	BP86[a]	Assign	BP86[a]	Assign	BP86[a]	Assign	BP86[a]	Assign	BP86[a]
1839.3	1854.7	ν_1 (a_1)	1870.1 (48)	ν_1 (a_1)	1871.8 (105)	ν_1 (a_1)	1845.9 (372)	ν_1 (a′)	1817.0 (181)	ν_1 (a′)	1834.4 (171)
1821.7	1835.3	ν_2 (a_1)	1824.2 (332)	ν_2 (a_1)	1699.8 (406)	ν_2 (a_1)	1797.2 (50)	ν_2 (a′)	1793.6 (137)	ν_2 (a′)	1810.7 (119)
1774.8		ν_3 (a_1)	660.4 (262)	ν_3 (a_1)	671.7 (364)	ν_3 (a_1)	708.8 (132)	ν_3 (a′)	1069.3 (236)	ν_3 (a′)	1785.7 (212)
728.1		ν_4 (a_1)	35.2 (0.08)	ν_4 (a_1)	118.6 (3)	ν_4 (a_1)	625.5 (313)	ν_4 (a′)	892.4 (26)	ν_4 (a′)	715.0 (46)
657.8	755.9	ν_5 (e)	1875.9 (136)	ν_5 (e)	1884.9 (125)	ν_5 (a_1)	120.7 (7)	ν_5 (a′)	670.3 (227)	ν_5 (a′)	673.6 (286)
		ν_6 (e)	726.6 (0.2)	ν_6 (e)	717.8 (38)	ν_6 (a_2)	614.9 (0)	ν_6 (a′)	648.2 (276)	ν_6 (a′)	544.4 (69)
		ν_7 (e)	687.5 (139)	ν_7 (e)	617.1 (47)	ν_7 (b_1)	1832.9 (160)	ν_7 (a′)	370.1 (15)	ν_7 (a′)	352.9 (22)
		ν_8 (e)	214.6 (0.2)	ν_8 (e)	167.2 (1)	ν_8 (b_1)	535.0 (48)	ν_8 (a′)	147.9 (0.1)	ν_8 (a′)	248.6 (1)
1830.6	1845.0					ν_9 (b_1)	204.1 (0.1)	ν_9 (a″)	1824.4 (147)	ν_9 (a″)	1818.8 (144)
720.3						ν_{10} (b_2)	1774.9 (52)	ν_{10} (a″)	713.8 (78)	ν_{10} (a″)	714.4 (55)
						ν_{11} (b_2)	669.8 (114)	ν_{11} (a″)	382.5 (7)	ν_{11} (a″)	332.4 (33)
						ν_{12} (b_2)	230.8 (2)	ν_{12} (a″)	290.6 (5)	ν_{12} (a″)	322.4 (0)

[a] Calculated using a BP86 functional in combination with a TZVPP basis set for Al and H and an ecp-TZVPP basis set for Sn.

Table 4. Experimental IR wavenumbers [cm^{-1}] of **1b** and **3b** and calculated wavenumbers [cm^{-1}] and intensities [$km\,mol^{-1}$, given in parentheses] of the four isomers of $Ga{\cdot}SnH_4$, **I–IV**, and $HGaSnH_3$, **V**.

Observed		$Ga{\cdot}SnH_4$ (**I**)		$Ga{\cdot}SnH_4$ (**II**)		$Ga{\cdot}SnH_4$ (**III**)		$Ga{\cdot}SnH_4$ (**IV**)		$HGaSnH_3$ (**V**)	
1b	**3b**	Assign	BP86[a]	Assign	BP86[a]	Assign	BP86[a]	Assign	BP86[a]	Assign	BP86[a]
1849.3	1839.4	ν_1 (a_1)	1863.3 (39)	ν_1 (a_1)	1873.1 (93)	ν_1 (a_1)	1844.7 (311)	ν_1 (a')	1802.5 (129)	ν_1 (a')	1821.7 (170)
1824.7		ν_2 (a_1)	1817.4 (353)	ν_2 (a_1)	1740.7 (433)	ν_2 (a_1)	1806.3 (70)	ν_2 (a')	1808.1 (181)	ν_2 (a')	1782.9 (140)
1734.4		ν_3 (a_1)	653.9 (266)	ν_3 (a_1)	671.7 (339)	ν_3 (a_1)	714.6 (86)	ν_3 (a')	1007.5 (31)	ν_3 (a')	1710.8 (298)
714.8		ν_4 (a_1)	20.1 (0.1)	ν_4 (a_1)	76.2 (0.8)	ν_4 (a_1)	646.7 (322)	ν_4 (a')	925.9 (224)	ν_4 (a')	701.6 (50)
650.4		ν_5 (e)	1867.4 (145)	ν_5 (e)	1884.8 (130)	ν_5 (a_1)	79.1 (1)	ν_5 (a')	667.2 (90)	ν_5 (a')	650.8 (355)
496.8		ν_6 (e)	725.1 (0.1)	ν_6 (e)	718.7 (37)	ν_6 (a_2)	620.0 (0)	ν_6 (a')	324.3 (21)	ν_6 (a')	487.8 (24)
		ν_7 (e)	684.6 (141)	ν_7 (e)	623.1 (53)	ν_7 (b_1)	1831.3 (161)	ν_7 (a')	643.7 (467)	ν_7 (a')	301.2 (17)
		ν_8 (e)	182.9 (0.05)	ν_8 (e)	158.9 (0.2)	ν_8 (b_1)	528.4 (60)	ν_8 (a')	82.1 (2)	ν_8 (a')	171.0 (0.8)
1835.3	1787.8					ν_9 (b_1)	129.6 (1)	ν_9 (a'')	1832.0 (147)	ν_9 (a'')	1793.8 (157)
724.8						ν_{10} (b_2)	1787.3 (70)	ν_{10} (a'')	716.0 (88)	ν_{10} (a'')	713.0 (57)
						ν_{11} (b_2)	675.8 (107)	ν_{11} (a'')	485.2 (16)	ν_{11} (a'')	328.7 (16)
						ν_{12} (b_2)	180.7 (1)	ν_{12} (a'')	270.0 (3)	ν_{12} (a'')	268.5 (9)

[a] Calculated using a BP86 functional in combination with a TZVPP basis set for Ga and H and an ecp-TZVPP basis set for Sn.

3b; the calculated dimensions are given in the Supporting Information (Table S1). Unlike **III**, the more stable isomer **IV** involves marked perturbation of one Sn–H bond, elongating it by some 23 pm and effectively establishing an Sn–H···M bridge. The result is that what approximates to a ν(Sn–H) mode is predicted to occur at unusually low wavenumber (e.g., 1069.3 cm^{-1} for the Al version of **IV**) and with high intensity in IR absorption. No absorption answering to this description could be discerned in the spectrum associated with either **1a**/**1b** or **3a**/**3b**, although none of the absorptions characteristic of **3a**/**3b** was observed more than weakly, so that the possibility of such a structure cannot so easily be discounted in this case. The IR spectrum calculated for **III** is dominated by four quite closely spaced absorptions of comparable intensity between 1770 and 1850 cm^{-1}, with others near 710, 670–680, 620–650 and 530 cm^{-1}. Although this matches quite closely the spectra of **1a** and **1b**, theory and experiment diverge in two particulars. Firstly, the intensity pattern of the four prominent bands observed in each case between 1730 and 1850 cm^{-1} differs significantly from the calculated pattern, such that the feature at lowest wavenumber (1774.8 or 1734.4 cm^{-1} for **1a** or **1b**, respectively) is, for example, the most intense of the four in practice, but the least intense in theory. Secondly, the H/D ratios and, most significantly, the Ga isotopic splitting in the Ga experiments leave little doubt that the transition at 1774.8 or 1734.4 cm^{-1} represents a vibration that approximates closely not to a ν(Sn–H) but to a ν(M–H) mode (M = Al or Ga). None of the models **I–IV** is able to accommodate this finding.

The experimental results give strong prima facie evidence therefore that in **1a** and **1b**, the main product formed on co-deposition of Al or Ga (M) vapor with SnH_4, the M atom has inserted into an Sn–H bond to give the M^{II} compound $HMSnH_3$ (**V**). This would then appear to occur spontaneously, despite the fact that the corresponding silane derivative is formed only on photoactivation at λ = ca. 254 or 410 nm.[14] Our DFT calculations show that $HMSnH_3$ (**V**) has a global minimum energy structure with C_s symmetry and the dimensions recorded in Table S1 (Supporting Information). With a $^2A'$ ground state and the unpaired electron localized largely at M, the molecule resembles other M^{II} hydrides in featuring an angular H-M-Sn skeleton ($\sphericalangle$H-Al-Sn = 117.7°, $\sphericalangle$H-Ga-Sn = 120.0°), compare with MH_2,[27] $HMCH_3$,[16] $HMSiH_3$,[14] $HMNH_2$,[32] and $HMPH_2$.[33] The calculated energy change, ΔE, for its formation from SnH_4 and an M atom in its ^2P ground electronic state [Eq. (2)] is −102.0 and −65.8 $kJ\,mol^{-1}$ for M = Al and Ga, respectively. Hence **V** lies 40–74 $kJ\,mol^{-1}$ lower than **IV** on the $MSnH_4$ energy hypersurface. The wavenumbers and IR intensities estimated for the vibrational fundamentals of $HAlSnH_3$ and $HGaSnH_3$ (**1a**/**1b**) in their normal and perdeuterated forms reveal patterns in good agreement with those of the corresponding versions of **1a** and **1b**, with four quite closely spaced absorptions expected at 1700–1840 cm^{-1}, as well as an intense absorption at 640–680 cm^{-1} (see Table 5). There seems little doubt therefore that **1a** and **1b** are indeed the insertion products $HAlSnH_3$ and $HGaSnH_3$ (**V**).

The case of **3a**/**3b** is more problematic. The spectroscopic signs are those that might be anticipated for a 1:1 adduct of the metal atom M with SnH_4. As already noted, however, there is no sign of an absorption in the range 900–1150 cm^{-1} to be expected of the most stable isomer **IV**. Although the isomer **III**, with the M atom directed toward an edge of the SnH_4 tetrahedron, would provide a rather better match for the spectra displayed by **3a** and **3b**, this seems to be an unlikely identity, given that it is calculated to be less stable than **IV**. More seriously, the photochemical properties of **3a**/**3b** which, unlike **1a**/**1b**, decays only on exposure to light of quite short wavelength ($\lambda \approx 410$ nm), run counter to those expected of a metal atom adduct M···SnH_4. Such an adduct is inevitably the precursor to the insertion product **V** the formation of which is evidently *opposed by little or no activation barrier*. Taking everything into account, we believe that **3a**/**3b** is indeed a loose aggregate of the type M···SnH_4, but inhibited from further reaction by the intercession of the rigid matrix environment. For example, M and SnH_4 may be not nearest but next nearest neighbors in the matrix. The calculations give some support to this notion in revealing quite strong interaction for an M···SnH_4 contact pair, so that even with the increased separation between M and SnH_4 enforced by the matrix, weak but significant interaction may be expected to persist. Only by exciting the metal atom by exposure to blue or near-UV light is sufficient

Table 5. Experimental IR wavenumbers [cm^{-1}] of **1a** and **1b** and calculated wavenumbers [cm^{-1}] and intensities [$km\,mol^{-1}$, given in parentheses] for $HMSnH_3$ and $DMSnD_3$ (**V**) (M = Al and Ga).

Assign	$HAlSnH_3$ (**V**)		$DAlSnD_3$ (**V**)		$HGaSnH_3$ (**V**)		$DGaSnD_3$ (**V**)	
	1a, obsd	calcd[a]	**1a**, obsd	calcd[a]	**1b**, obsd	calcd[a]	**1b**, obsd	calcd[a]
ν_1 (a′)	1839.3	1834.4 (171)	1321.6	1303.4 (100)	1849.3	1823.6 (168)	1328.5/1320.4	1295.3 (88)
ν_2 (a′)	1821.7	1810.7 (119)	1307.9	1288.7 (61)	1824.7	1778.0 (142)	1288.4	1260.7 (70)
ν_3 (a′)	1774.8	1785.7 (212)	1292.6	1281.0 (99)	1734.4	1710.7 (298)	1253.3	1219.0 (152)
ν_4 (a′)	728.1	715.0 (46)		507.4 (24)	714.8	702.1 (50)	511.0	498.2 (25)
ν_5 (a′)	657.8	673.6 (286)	471.5	480.8 (143)	650.4	652.3 (355)	469.2/466.2	466.1 (179)
ν_6 (a′)		544.4 (69)		400.1 (39)	496.8	487.4 (24)		352.2 (13)
ν_7 (a′)		352.9 (22)		258.9 (8)		304.0 (17)		216.8 (9)
ν_8 (a′)		248.6 (1)		237.8 (4)		171.1 (0.8)		169.7 (0.9)
ν_9 (a″)	1830.6	1818.8 (144)	1316.2	1292.8 (74)	1835.3	1788.8 (158)	1309.3/1301.0	1271.9 (81)
ν_{10} (a″)	720.3	714.4 (55)		507.2 (28)	724.8	713.7 (57)	516.1	506.9 (29)
ν_{11} (a″)		332.4 (33)		236.0 (17)		329.5 (16)		234.1 (8)
ν_{12} (a″)		322.4 (0)		235.3 (0)		270.4 (9)		194.8 (5)

[a] Calculated using a BP86 functional in combination with a TZVPP basis set for Al, Ga and H and an ecp-TZVPP basis set for Sn.

energy imparted to overcome the constraints of the matrix environment and promote reaction. Under circumstances in which **1a**/**1b** is highly photolabile, this reaction proceeds with the formation of **2a**/**2b**.

$H_2M(\mu\text{-}H)_2Sn$ (VI; M = Al or Ga): Earlier studies of matrix reactions of Al or Ga atoms (M) with simple hydride molecules, HX, have revealed that photoactivation at wavelengths near 400 nm results in insertion to give a M^{II} hydride HMX, for example, X = NH_2[32] or OH;[43] broad-band UV-visible photolysis then results typically in decomposition to H· + MX. Insertion having already occurred on co-deposition with SnH_4, the course taken on subsequent photolysis at λ = 400–800 nm, with the conversion of $HMSnH_3$ (**V**) to **2a**/**2b** comes as a surprise. The fact that **2a** is actually formed to some extent even on deposition of the matrix is most probably due to photolysis by radiation emitted by the metal furnace. In fact, the IR spectra characterizing **2a**/**2b** have little in common with that to be expected of a subvalent M[14,16,27,32,33] or tin[20] hydride. For example, it shows no sign of the stretching vibrations of the terminal M–H or Sn–H bonds normally associated with such species. What appear to be the defining properties of the spectra are the bands at 1100–1420 and 1870–1970 cm^{-1}, which bear the marks of one or more metal–hydrogen–metal bridges[28–30,40,41] and terminal M^{III}–H bonds,[26,27,32,38,39,44] respectively. Since **2a**/**2b** is formed from **V**, it must be assumed that there is no increase in nuclearity with regard to the metal atoms, and the failure to detect any known binary hydrides of M or Sn makes it most likely that **2a**/**2b** is an isomer of **V**.

The only model for **2a**/**2b** that is consistent with the experimental findings is $H_2M(\mu\text{-}H)_2Sn$ (**VI**), a novel mixed-metal hydride, remarkable as much for the implied oxidation states of the metals as for its structure. Our DFT calculations find a well-defined minimum for such a molecule with the geometry **VI** illustrated in Figure 8. The ground state is a doublet with C_{2v} molecular symmetry. One plane of symmetry contains the planar $M(\mu\text{-}H)_2Sn$ skeleton with M–H and Sn–H distances of 176.0 and 197.0 pm for M = Al and of 175.5 and 198.1 pm for M = Ga, while the second, perpendicular to the first, contains the terminal M–H bonds each measuring 159.2 and 156.4 pm for M = Al and Ga, respectively. The angles (in the order Al/Ga; br = bridging, t = terminal) are as follows: H_{br}-Sn-H_{br} 73.2/72.8°; H_{br}-M-H_{br} 83.8/84.2°; H_t-M-H_t 124.8/127.8°. The energy change, ΔE, then calculated for the formation of **VI** from $M(^2P)$ and SnH_4 [Eq. (5)] is −200.8 or −125.7 $kJ\,mol^{-1}$ according to whether M = Al or Ga, so that this appears to correspond to the global minimum on the $MSnH_4$ PE hypersurface, being more stable than **V** (Al/Ga) by 98.8 and 59.9 $kJ\,mol^{-1}$, respectively.

$$M(^2P) + SnH_4 \rightarrow H_2M(\mu\text{-}H)_2Sn \quad (\mathbf{VI}) \qquad (5)$$

The wavenumbers and IR intensities calculated for the vibrational fundamentals of the normal and perdeuterated isotopomers of **VI** match remarkably closely those of the IR features observed for the corresponding versions of **2a**/**2b**. Indeed, the calculations reproduce the wavenumbers of the 17 fundamentals that appear to have been located experimentally for $H_2Ga(\mu\text{-}H)_2Sn$ and $D_2Ga(\mu\text{-}D)_2Sn$ with a root mean square deviation of no more than 2.4% (see Table 6).

Hence experiment and theory combine to suggest that photolysis with light at wavelengths of 400–800 nm results in the tautomerization of $HMSnH_3$ (**V**) to $H_2M(\mu\text{-}H)_2Sn$ (**VI**). The net outcome is a redox reaction in which the M atom has ultimately been oxidized to M^{III}, while the tin atom has been formally reduced to the unusual state of Sn^I. The only comparable Sn^I species to have been identified previously is SnH. Although short-lived in the gas phase,[45] this can be preserved, as can its dimer $Sn(\mu\text{-}H)_2Sn$ apparently, under matrix conditions.[20] The DFT calculations confirm, as expected, that the unpaired electron in $H_2M(\mu\text{-}H)_2Sn$ (**VI**) occupies an orbital that is localized mainly on the Sn atom. Perhaps the closest analogy to this product is provided by H_2MPH, another M^{III} radical species, which is formed together with $HMPH_2$ in an Ar matrix on photolysis of the adduct M···PH_3 at $\lambda \approx 436$ nm.[33] The response of SnH_4 to the Group 13 metal atoms contrasts in this respect with its response under similar conditions to Ti atoms which, with minimal activation, gives rise to the triply hydrogen-bridged product $HTi(\mu\text{-}H)_3Sn$.[46] Exchange of hydrogen between one metal or metalloid center and another is also known to

Table 6. Experimental IR wavenumbers [cm^{-1}] of **2a** and **2b** and calculated wavenumbers [cm^{-1}] and intensities [$km\,mol^{-1}$, given in parentheses] for $H_2M(\mu\text{-}H)_2Sn$ and $D_2M(\mu\text{-}D)_2Sn$ (**VI**) (M = Al and Ga).

Assign	$H_2Al(\mu\text{-}H)_2Sn$ (**VI**)		$D_2Al(\mu\text{-}D)_2Sn$ (**VI**)		$H_2Ga(\mu\text{-}H)_2Sn$ (**VI**)		$D_2Ga(\mu\text{-}D)_2Sn$ (**VI**)	
	2a, obsd	calcd[a]	**2a**, obsd	calcd[a]	**2b**, obsd	calcd[a]	**2b**, obsd	calcd[a]
ν_1 (a_1)	1878.1	1882.8 (106)		1341.5 (71)	1934.3	1922.4 (108)	1375.7	1363.1 (59)
ν_2 (a_1)	1400.1	1420.1 (331)	1010.3	1012.5 (199)	1389.6	1400.0 (216)	1008.6	992.5 (115)
ν_3 (a_1)	1209.6	1258.5 (722)	922.7	894.7 (357)	1144.1	1192.8 (799)	830.9	846.9 (404)
ν_4 (a_1)	732.9	727.1 (311)	534.8	528.3 (153)	704.8	688.3 (306)	505.6	491.3 (153)
ν_5 (a_1)		261.5 (0)		253.0 (1)		186.0 (0.01)		184.7 (0.03)
ν_6 (a_2)		575.1 (0)		406.9 (0)		578.8 (0)		409.5 (0)
ν_7 (b_1)		1896.9 (183)	1390.1	1377.9 (103)	1954.8	1936.3 (176)	1390.9	1384.3 (92)
ν_8 (b_1)	611.5	615.2 (64)		447.7 (32)	615.7	585.7 (45)	438.2	420.5 (23)
ν_9 (b_1)		323.4 (2)		230.7 (1)		245.7 (0.2)		174.8 (0.1)
ν_{10} (b_2)	1271.4	1264.8 (45)		898.1 (16)	1221.2	1213.2 (14)	882.7/867.8	859.3 (6)
ν_{11} (b_2)	1129.1	1140.3 (179)	889.1	818.7 (102)	1122.0	1105.2 (155)	811.1	787.2 (80)
ν_{12} (b_2)	541.2	558.9 (63)		412.4 (32)	514.0	517.6 (22)		374.3 (11)

[a] Calculated using a BP86 functional in combination with a TZVPP basis set for Al, Ga and H and an ecp-TZVPP basis set for Sn.

occur in certain chemical vapor deposition processes involving, for example, MMe_3 (M = Ga or In) and $Me_3N{\cdot}AlH_3$.[47]

$Ga_2(\mu\text{-}H)_4Sn$ (VIII; 4b): The product **4b** is formed on co-deposition of Ga vapor with SnH_4 in yields that vary with the reagent concentrations in such a way as to suggest that its source is $Ga_2 + SnH_4$ [see Eq. (4), for example]. Parallels are then evident with similar matrix experiments involving Ga vapor and H_2,[30] H_2O,[43] or SiH_4.[14] Ga_2 reacts spontaneously with H_2 to form the cyclic molecule $Ga(\mu\text{-}H)_2Ga$,[30,48] whereas with SiH_4 it forms, again spontaneously, what is probably the product $HGa(\mu\text{-}SiH_3)Ga$.[14] Several possible models for **4b** commend themselves, for example, $Ga(\mu\text{-}H)(\mu\text{-}SnH_3)Ga$, $Ga(\mu\text{-}H)GaSnH_3$, $HGa(\mu\text{-}SnH_3)Ga$, as well as $GaGa(H)SnH_3$ and *trans*-$HGaGaSnH_3$ with terminal H and SnH_3 ligands bound either to the same or to different Ga atoms of a diatomic Ga_2 unit (cf. $GaGaH_2$ and HGaGaH which have been identified in earlier experiments[30]). The only minima on the $GaGaSnH_4$ energy hypersurface correspond, on the evidence of our DFT calculations, to $GaGa(H)SnH_3$ (**VII**) with terminal Ga–H and Ga–SnH_3 bonds and a novel hydrogen-bridged metal cluster, namely the armchair-shaped isomer **VIII** (see Figure 8). Although this second molecule can be regarded as an adduct of $Ga(\mu\text{-}H)_2Ga$[30] and SnH_2, the hydrogen atoms establish comparable contacts to all the metal atoms which they bridge (at distances ranging from 183 to 229 pm; see Table S2, Supporting Information), and the molecule is perhaps viewed more aptly as a metal-deficient cubanelike cluster. The single IR absorption at 1180.3 cm^{-1} by which **4b** is recognizable clearly implies a molecule featuring a bridging Ga-H-Ga or Ga-H-Sn unit. This circumstance declares isomer **VIII**, but not **VII**, to be a reasonable candidate for **4b**. According to the calculations, the vibrational transitions of **VIII** predicted to be most intense in IR absorption occur at 1363.6, 1321.8, and 1255.7 cm^{-1} (Table S2, Supporting Information). The formation energies starting from two metal atoms and one SnH_4 molecule are −249.7 and −315.5 $kJ\,mol^{-1}$ for **VII** and **VIII**, respectively, making the latter 65.8 $kJ\,mol^{-1}$ more stable than the former. On the very limited experimental evidence available, **VIII** seems therefore to be the most likely product of the facile reaction between Ga_2 and SnH_4. Further experiments are in progress to test this conclusion and seek a more detailed characterization of the product.

Effect of broad-band UV-visible photolysis: Less discriminate irradiation with broad-band UV-visible light (λ = 200–800 nm) brings about the photodecomposition of all the species **1a**/**1b**, **2a**/**2b**, **3a**/**3b**, and **4b**, without giving rise to any new IR absorptions of significant intensity. Although H· atoms or H_2 might have been expected to be eliminated under these conditions, it seems rather unlikely that these would not be accompanied by the formation of known hydrides of the metals, such as MH[27] and SnH_n (n = 1–3),[20] or unknown but potentially detectable ones such as $MSnH_3$. The most likely explanation is that regeneration of M atoms or M_2 dimers and SnH_4 [i.e., reversal of reactions in Eqs. (1), (2), (4), and (5)] occurs under these circumstances.

Acknowledgement

The authors thank 1) the EPSRC for financial support of the Oxford group, including the funding of a research studentship for V.A.M. and of a research assistantship for J.A.J.P., and 2) the Deutsche Forschungsgemeinschaft and the Fonds der Chemischen Industrie for similar support of the Karlsruhe group.

[1] a) R. H. Crabtree, *Chem. Rev.* **1985**, *85*, 245; b) U. Schubert, *Adv. Organomet. Chem.* **1990**, *30*, 151; c) R H. Crabtree, *Angew. Chem.* **1993**, *105*, 828; *Angew. Chem. Int. Ed. Engl.* **1993**, *32*, 789; d) C. Hall, R. N. Perutz, *Chem. Rev.* **1996**, *96*, 3125; e) J. Y. Corey, J. Braddock-Wilking, *Chem. Rev.* **1999**, *99*, 175; f) Z. Lin, *Chem. Soc. Rev.* **2002**, *31*, 239.

[2] H. C. Lo, A. Haskel, M. Kapon, E. Keinan, *J. Am. Chem. Soc.* **2002**, *124*, 3226.

[3] I. Atheaux, B. Donnadieu, V. Rodriguez, S. Sabo-Etienne, B. Chaudret, K. Hussein, J.-C. Barthelat, *J. Am. Chem. Soc.* **2000**, *122*, 5664.

[4] U. Schubert, E. Kunz, B. Harkers, J. Willnecker, J. Meyer, *J. Am. Chem. Soc.* **1989**, *111*, 2572.

[5] H. Piana, U. Kirchgässner, U. Schubert, *Chem. Ber.* **1991**, *124*, 743.

[6] a) M. J. Almond, A. J. Downs, *Adv. Spectrosc.* **1989**, *17*, 1; b) I. R. Dunkin, *Matrix-Isolation Techniques: A Practical Approach*, Oxford University Press, Oxford, **1998**.

[7] H.-J. Himmel, A. J. Downs, T. M. Greene, *Chem. Rev.* **2002**, *102*, 4191.

[8] D. R. Meininger, B. S. Ault, *J. Phys. Chem. A* **2000**, *104*, 3481.
[9] S. R. Davis, L. Andrews, *J. Phys. Chem.* **1989**, *93*, 1273.
[10] Z. Mielke, K. G. Tokhadze, *Chem. Phys. Lett.* **2000**, *316*, 108.
[11] V. A. Macrae, T. M. Greene, A. J. Downs, *J. Phys. Chem. A* **2004**, *108*, 1393.
[12] a) M. A. Lefcourt, G. A. Ozin, *J. Am. Chem. Soc.* **1988**, *110*, 6888; b) M. A. Lefcourt, G. A. Ozin, *J. Phys. Chem.* **1991**, *95*, 2616.
[13] B. Gaertner, H.-J. Himmel, *Angew. Chem.* **2002**, *114*, 1602; *Angew. Chem. Int. Ed.* **2002**, *41*, 1538.
[14] B. Gaertner, H.-J. Himmel, V. A. Macrae, A. J. Downs, T. M. Greene, *Chem. Eur. J.* **2004**, *10*, 3430.
[15] See, for example: A. Zumbusch, H. Schnöckel, *J. Chem. Phys.* **1998**, *108*, 8092.
[16] H.-J. Himmel, A. J. Downs, T. M. Greene, L. Andrews, *Organometallics* **2000**, *19*, 1060.
[17] A. E. Finholt, A. C. Bond, Jr., K. E. Wilzbach, H. I. Schlesinger, *J. Am. Chem. Soc.* **1947**, *69*, 2692.
[18] H. Bürger, A. Rahner, *Vib. Spectra Struct.* **1990**, *18*, 217.
[19] a) R. Ahlrichs, M. Bär, M. Häser, H. Horn, C. Kölmel, *Chem. Phys. Lett.* **1989**, *162*, 165; b) K. Eichkorn, O. Treutler, H. Öhm, M. Häser, R. Ahlrichs, *Chem. Phys. Lett.* **1995**, *240*, 283; c) K. Eichkorn, O. Treutler, H. Öhm, M. Häser, R. Ahlrichs, *Chem. Phys. Lett.* **1995**, *242*, 652; d) K. Eichkorn, F. Weigend, O. Treutler, R. Ahlrichs, *Theor. Chem. Acc.* **1997**, *97*, 119; e) F. Weigend, M. Häser, *Theor. Chem. Acc.* **1997**, *97*, 331; f) F. Weigend, M. Häser, H. Patzelt, R. Ahlrichs, *Chem. Phys. Lett.* **1998**, *294*, 143.
[20] X. Wang, L. Andrews, G. V. Chertihin, P. F. Souter, *J. Phys. Chem. A* **2002**, *106*, 6302.
[21] a) G. P. Ayers, A. D. E. Pullin, *Spectrochim. Acta A* **1976**, *32*, 1629; b) L. Fredin, B. Nelander, G. Ribbegård, *J. Chem. Phys.* **1977**, *66*, 4065.
[22] H. Dubost, *Chem. Phys.* **1976**, *12*, 139.
[23] a) L. Fredin, B. Nelander, G. Ribbegård, *J. Mol. Spectrosc.* **1974**, *53*, 410; b) R. Guasti, V. Schettino, N. Brigot, *Chem. Phys.* **1978**, *34*, 391.
[24] C. Xu, L. Manceron, J. P. Perchard, *J. Chem. Soc. Faraday Trans.* **1993**, *89*, 1291.
[25] L. Andrews, T. R. Burkholder, J. T. Yustein, *J. Phys. Chem.* **1992**, *96*, 10182.
[26] S. Aldridge, A. J. Downs, *Chem. Rev.* **2001**, *101*, 3305.
[27] P. Pullumbi, C. Mijoule, L. Manceron, Y. Bouteiller, *Chem. Phys.* **1994**, *185*, 13, 25.
[28] a) L. Andrews, X. Wang, *Science* **2003**, *299*, 2049; b) X. Wang, L. Andrews, S. Tam, M. E. DeRose, M. E. Fajardo, *J. Am. Chem. Soc.* **2003**, *125*, 9218.
[29] A. S. Grady, S. G. Puntambekar, D. K. Russell, *Spectrochim. Acta A* **1991**, *47*, 47.
[30] H.-J. Himmel, L. Manceron, A. J. Downs, P. Pullumbi, *J. Am. Chem. Soc.* **2002**, *124*, 4448.
[31] J. M. Parnis, G. A. Ozin, *J. Phys. Chem.* **1989**, *93*, 1204, 1220.
[32] H.-J. Himmel, A. J. Downs, T. M. Greene, *J. Am. Chem. Soc.* **2000**, *122*, 9793.
[33] H.-J. Himmel, A. J. Downs, T. M. Greene, *Inorg. Chem.* **2001**, *40*, 396.
[34] J. H. Ammeter, D. C. Schlosnagle, *J. Chem. Phys.* **1973**, *59*, 4784.
[35] R. Grinter, R. J. Singer, *Chem. Phys.* **1987**, *113*, 87.
[36] M. A. Douglas, R. H. Hauge, J. L. Margrave, *J. Phys. Chem.* **1983**, *87*, 2945.
[37] See, for example: a) M. Poliakoff, J. J. Turner, *J. Chem. Soc. Dalton Trans.* **1973**, 1351; b) M. Fanfarillo, H. E. Cribb, A. J. Downs, T. M. Greene, M. J. Almond, *Inorg. Chem.* **1992**, *31*, 2962.
[38] R. Köppe, H. Schnöckel, *J. Chem. Soc. Dalton Trans.* **1992**, 3393.
[39] A. J. Downs, T. M. Greene, E. Johnsen, P. T. Brain, C. A. Morrison, S. Parsons, C. R. Pulham, D. W. H. Rankin, K. Aarset, I. M. Mills, E. M. Page, D. A. Rice, *Inorg. Chem.* **2001**, *40*, 3484.
[40] C. R. Pulham, A. J. Downs, M. J. Goode, D. W. H. Rankin, H. E. Robertson, *J. Am. Chem. Soc.* **1991**, *113*, 5149.
[41] P. L. Baxter, A. J. Downs, M. J. Goode, D. W. H. Rankin, H. E. Robertson, *J. Chem. Soc. Dalton Trans.* **1990**, 2873.
[42] *CRC Handbook of Chemistry and Physics, 84th ed.* (Ed.: D. R. Lide), CRC, Boca Raton, FL, **2003**–**2004**.
[43] a) R. H. Hauge, J. W. Kauffman, J. L. Margrave, *J. Am. Chem. Soc.* **1980**, *102*, 6005; b) A. J. Downs, V. A. Macrae, *Phys. Chem. Chem. Phys.* **2004**, in press.
[44] H.-J. Himmel, C. Klaus, *Z. Anorg. Allg. Chem.* **2003**, *629*, 1477.
[45] W. Zimmermann, U. Simon, M. Petri, W. Urban, *Mol. Phys.* **1991**, *74*, 1287.
[46] A. Bihlmeier, T. M. Greene, H.-J. Himmel, *Organometallics* **2004**, *23*, 2350.
[47] See, for example: A. C. Jones, P. O'Brien, *CVD of Compound Semiconductors: Precursor Synthesis, Development and Applications*, VCH, Weinheim (Germany), **1997**, pp. 125, 140.
[48] A. Köhn, H.-J. Himmel, B. Gaertner, *Chem. Eur. J.* **2003**, *9*, 3909.

Received: June 7, 2004
Published online: October 13, 2004

